Leadership in Sustainable Infrastructure

Leadership en Infrastructures Durables

Vancouver, Canada

May 31 – June 3, 2017/ *Mai 31 – Juin 3, 2017*

COMPLEX LOAD SHARING IN WEAK-AXIS MOMENT CONNECTIONS OF INDUSTRIAL STEEL STRUCTURES

Quintin, Riley[1], Driver, Robert[1] and Callele, Logan[2]

[1] Department of Civil and Environmental Engineering, University of Alberta, Edmonton, Canada

[2] Waiward Steel LP, Edmonton, Canada

Abstract: It has become common for steel fabricators to find torsional loads specified in design documents for industrial steel structures. These loads arise at beam-to-column moment connections whenever a beam is subjected to weak-axis bending, which is transferred to the supporting column as torsion. Due to a lack of codified guidelines or relevant literature on how to design the joint to transfer the torsional moment, engineers routinely add full-depth stiffeners to the column to prevent localized distortion of the cross-section, which is both costly and time consuming. Previous research at the University of Alberta investigated the behaviour of unstiffened wide-flange members subjected to torsion applied through one flange, and this research aims to extend that work to determine the impact of column axial load on this connection type. A parametric study using finite element simulations has been conducted to identify the major parameters affected by the presence of axial load. The parametric study considered variations in cross-sectional geometry and axial load. Preliminary results suggest that the length of an unstiffened column effective in resisting the applied torque does not change significantly with the presence of axial load. However, the bending stress at first yield is inversely related to the level of axial stress. Using these results, a design method will be proposed that predicts the maximum torsional moment that can be applied to an unstiffened wide-flange member before yielding occurs on the cross-section. This will improve the efficiency, constructability, and cost effectiveness of many industrial steel structures.

1 Introduction

The increased size and complexity of industrial structures throughout Canada, coupled with a labour-dominated market, has pushed both structural consultants and fabricators to design lighter and cheaper structures. Additional challenges arise due to complex load combinations caused by environmental loads, machine operation, design hydraulic events, future repurposing, as well as many other industrial loading scenarios. Structural behaviour is complex under multiple types of loading, and in some cases there is limited relevant literature or codified guidelines on how to design for these forces. Axial load and torsion is one load combination that is not well understood.

When members are called upon to resist multiple types of loading, wide-flange sections are often required to resist these forces due to their common use when in-plane flexural loads or axial compression dominate the behaviour. Their geometry also permits the use of simple, cost-effective connections that improve efficiency during erection. When wide-flange members are subjected to torsion, it is commonly applied by adjoining members that are connected to one flange only. This has led to the routine addition of full-depth stiffeners to the connection to ensure there is no localized distortion of the cross-section, which leads to increased fabrication time and cost. To eliminate the use of unnecessary stiffeners, it is necessary to establish the behaviour of unstiffened wide-flange members subjected to axial load and torsion applied through one flange.

A situation where the forces described above can be significant is shown in Figure 1, which depicts a modular pipe rack structure often used for heavy industrial building projects. The wide-flange beams that support the pipe are connected to wide-flange columns using moment connections. Design hydraulic events in the pipe cause weak-axis bending in the supporting beam to be transferred to the column as torsion. Multi-level pipe racks and the superimposed pipe loads mean the column section is likely carrying significant axial load when the hydraulic event occurs. As the torsional moment is applied to one flange of the column, localised deformations on the cross-section can cause local rotation of the flange that is not accounted for by classical elastic torsion theory, which may only be applied when the entire cross-section undergoes uniform rotation.

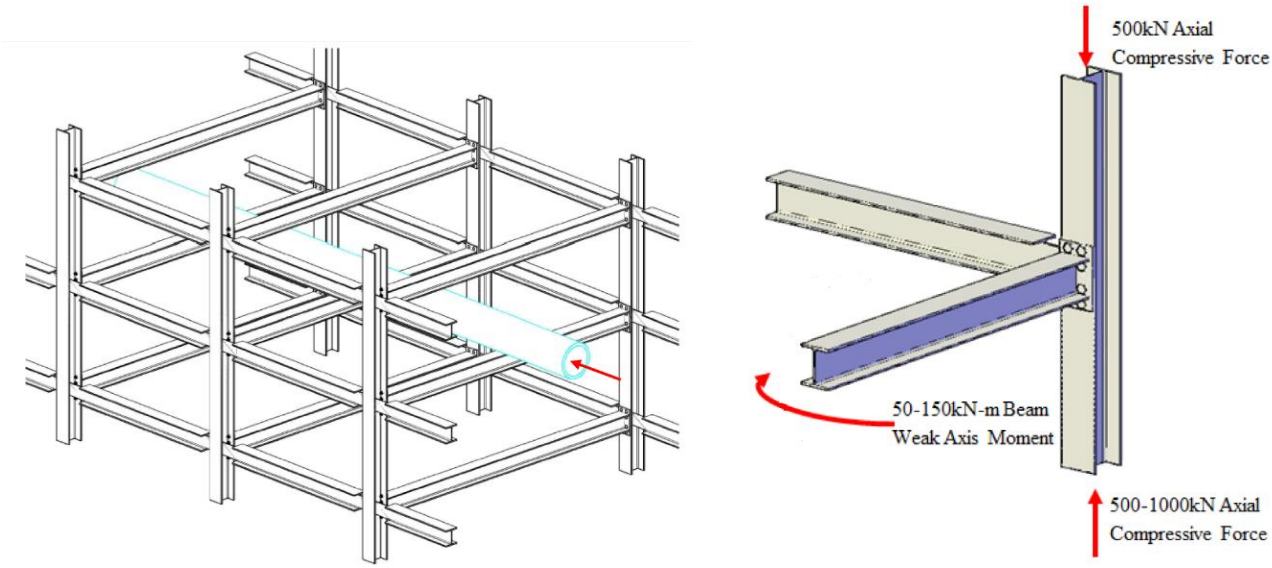

Figure 1: Pipe Rack Loading Example (Ahmad et al. 2016)

2 Previous Research

Recent research at the University of Alberta investigated the behaviour of wide-flange members subjected to torsion applied through one flange, but did not consider the presence of axial load. Through a series of parametric finite element simulations and full-scale laboratory testing, Ahmad et al. (2016) suggested the major resistance mechanism to this type of loading is a combination of web bending and torsion of the flange. They used a simple beam analogy to describe the localised bending strength and stiffness of the column web, as shown in Figure 2.

The web of the wide-flange section is treated as a simply-supported beam with a concentrated moment at one end and restrained by a spring that provides a semi-rigid rotational boundary condition at the other. Initial yielding on the cross-section will occur simultaneously on both sides of the web surface when the bending stress caused by the torsional moment reaches the yield stress of the material. Equations 1 – 4 detail the strength and stiffness of the column web based on the above idealization.

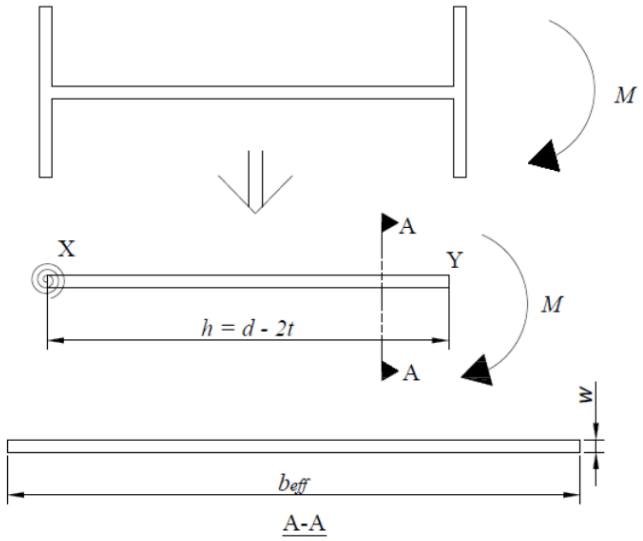

Figure 2: Beam Analogy for Web Bending Strength and Stiffness (Ahmad et al. 2016)

Equation 1 predicts the applied moment at the point of first yielding of the cross-section, which takes place on the surface of the web where the torque is applied. The torsional moment is resisted through a triangular (elastic) stress block whose height is equal to the yield stress of the material and width is the length of web effective in resisting the applied torque. The additional restraint provided by the flange in torsion is taken into account indirectly by the effective width term. As the torsional stiffness of the flange increases, a larger length of web is mobilized to resist the applied torque, resulting in a higher moment capacity.

$$[1]\ M_y = \frac{F_y b_{eff} w^2}{6}$$

M_y = maximum applied moment at first yield
b_{eff} = effective width of web that resists applied torque
w = web thickness
F_y = yield stress

$$[2]\ b_{eff} = N + r_1$$

N = connection length
r_1 = ratio of torsional stiffness of flange to bending stiffness of web

$$[3]\ r_1 = \frac{bt^3}{w^3}$$

b = flange width
t = flange thickness

$$[4]\ K_w = \frac{3.3E}{h}\left[(N+1.5r_1)\left(\frac{w^3}{12}\right)\right]$$

K_w = bending stiffness of web
E = Young's modulus
H = web height

Equation 4 describes the localised bending stiffness of the web; the effective width has been calibrated to the results of full-scale laboratory tests. The overall connection response is a combination of the localised web stiffness and the overall torsional stiffness of the member.

Ahmad et al. (2016) studied the impact of axial load on these sections through numerical analysis. Under varying levels of axial load, the elastic stiffness remained effectively constant, while the post-yield rotation was more severe at high levels of axial load, as shown in Figure 3.

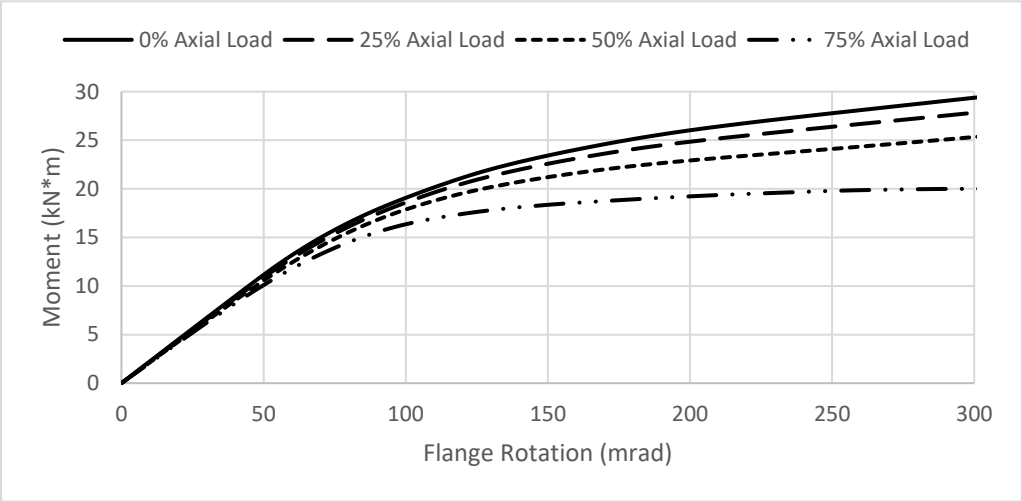

Figure 3: Moment–Rotation Response of a W310x97

An alternative equation (Ahmad et al. 2016) was suggested to predict the yield moment on the web that applies a von Mises interaction of stresses. It accounts for axial load by replacing the yield stress in Equation 1 with a reduced bending stress to account for all stress components defined in the von Mises equation. The assumed stress interaction is shown in Figure 4.

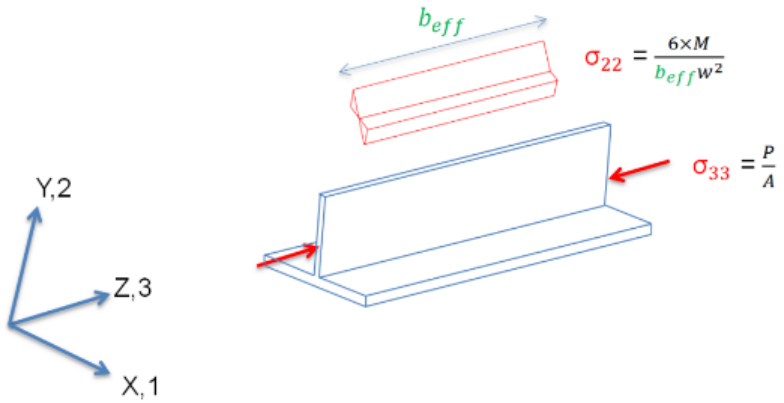

Figure 4: Stress Interaction from Combined Loading (Ahmad et al. 2016)

Given the coordinate system shown, the only non-zero components in the von Mises equation are the bending stress from the applied torsional moment (σ_{22}), and the axial compressive stress (σ_{33}). Setting the von Mises stress equal to the yield stress of the material and solving for the moment leads to Equation 5.

$$[5]\ M_y = \left| \frac{\frac{P}{A} - \sqrt{4F_y^2 - 3\left(\frac{P}{A}\right)^2}}{2} \right| \frac{b_{eff} w^2}{6}$$

P = applied axial force
A = cross-sectional area of wide-flange section

Ahmad et al. (2016) compared the yield moment predicted by Equation 5 with the results of 96 numerical models. Variations in applied axial load, length, and cross-sectional geometry were considered in the parametric study, which showed a consistent reduction in yield moment as the axial load increased. They also found that Equation 5 under-predicted the yield moment by increasing amounts as the axial force increased. At an axial stress equal to 75% of the nominal yield capacity of the member, the yield moment was underestimated by up to 20% using Equation 5. A more refined equation is needed that consistently predicts the strength of wide-flange sections under any level of axial load.

3 PARAMETRIC STUDY

To pinpoint the major factor(s) causing inaccuracy in Equation 5, as compared to the finite element simulations, the equation was separated into three distinct parts that were analyzed individually:

1. Effective Width - Based solely on geometric properties of the wide-flange column and the connection length, this parameter defines the width of the effective stress block. The effective width is considered constant, regardless of the level of axial stress.

2. Bending Stress - The term bound in absolute values represents the bending stress that develops at first yield. This value is affected by the material yield stress and applied axial load; it assumes only two components in the von Mises equation impact the bending stress at first yield.

3. Stress Distribution – In the final term, $w^2/6$, comes from the assumption that the stress distribution is linear through the thickness of the web.

It was noted from the results of previous research that variations in member length and cross-sectional geometry, such as flange width, flange thickness, member depth, and web thickness did not consistently influence the degradation in moment capacity under different levels of axial load. Standard sections have been modelled with axial loads ranging from 0 – 75% of their nominal axial yield capacity. The sections were chosen to represent a large variation in effective width to obtain a wide range of behaviours.

3.1 Finite Element Modelling

The finite element model was created using ABAQUS software. It has been modified from the model used in the study by Ahmad et al. (2016) to include the addition of axial load. Under pure torsion applied through one flange, this model has been verified using the results of full-scale laboratory tests. The full assembly of a 4 m-long W250x89 section is shown in Figure 5. All models were created using linear brick elements with full integration.

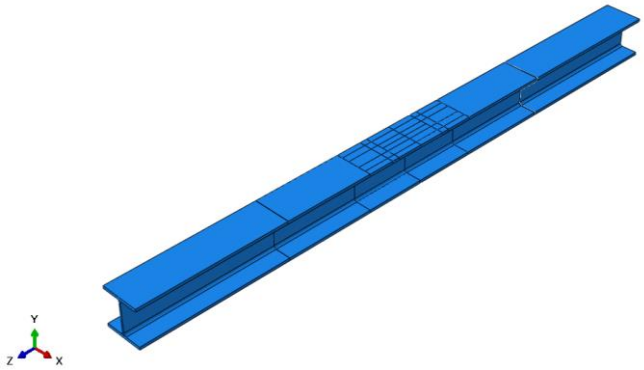

Figure 5: ABAQUS Finite Element Model Geometry

3.2 Material Properties

The material model assumes isotropic elasto-plastic behaviour with a Young's modulus of 200,000 MPa and Poisson's ratio of 0.3. A yield stress of 350 MPa was specified. Identification of first yield on the web surface was done using the PEEQ function in ABAQUS, where a non-zero value indicates the presence of plastic strain.

3.3 Loading

The wide-flange column is loaded in two separate, static general steps. The axial load is applied in four stages, where each stage applies one quarter of the total force. Compression is applied as a concentrated force to a reference point at the end of the wide flange section in the z-direction (Figure 5). To avoid localised distortion under the concentrated force, a rigid body tie constraint was applied to all nodes on the cross-section at the loaded end of the member. By tying these nodes to the reference point where the load was applied, the axial force is evenly applied over the entire cross-section.

The final loading step holds the axial stress constant while applying small increments of torsional moment to allow precise identification of first yield. The torsional moment was applied mid-span on the wide flange section through four pressure loads, as shown in Figure 6. By reversing the direction of the pressure load on either side of the web, a coupled moment is developed at the flange–web junction to simulate the torsional moment caused by weak-axis bending of an adjoining member. Pressure loads remain perpendicular to the surface they were applied to, meaning that as the flange rotates, the pressure loads continue to apply pure moment. Applying the torsional moment through a series of pressure loads was compared to a full model assembly consisting of a complete weak-axis moment connection and the response of the two models was found to be virtually the same. To reduce computational time and effort, this method of applying the torsional moment has been adopted for all finite element models.

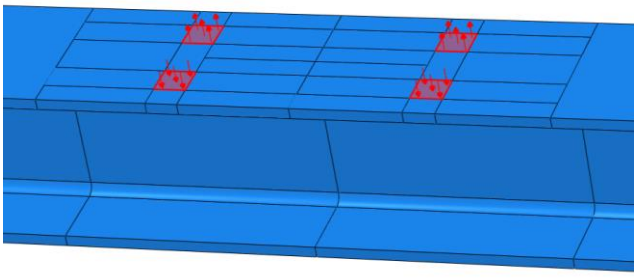

Figure 6: Simplified Torsional Loading

3.4 Boundary Conditions

The end restraints were chosen to simulate torsionally fixed boundary conditions. It is unlikely warping displacements would develop at the ends of the column given the large axial load. This was achieved in ABAQUS by restraining the nodes on the cross-section at both ends from displacement and rotation in all directions. Longitudinal displacement was permitted at the end where the load was applied to transfer the axial force into the column.

3.5 Mesh Optimization

The response of a wide-flange member subjected to a torsional moment applied to one flange is most sensitive to variations in web thickness. It was apparent through comparison to laboratory test results that further mesh refinement was needed beyond what was used in previous research. Using results from the full-scale testing program performed by Ahmad et al. (2016), the number of elements through the web thickness was progressively increased until there was no notable change to the yield moment, as shown in Figure 7. The final mesh used for this study utilized eight elements through the thickness of the web with full integration.

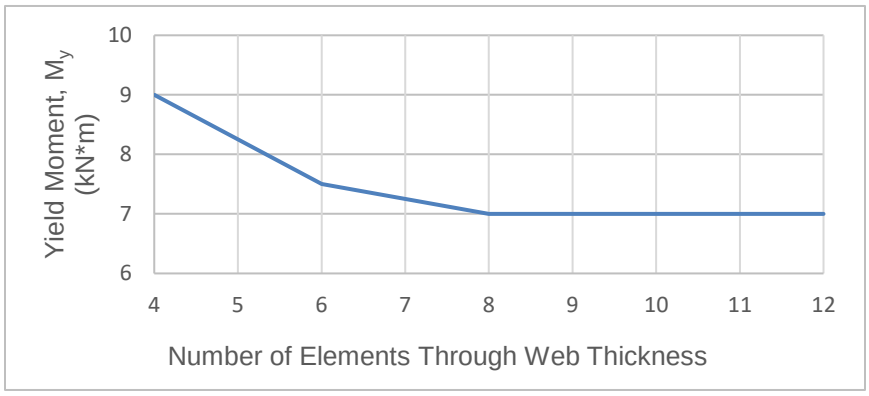

Figure 7: Mesh Convergence for a W310x67

4 RESULTS

A total of 32 numerical simulations were conducted. Seven different geometries were tested with an axial load ranging from 0 – 75% of the nominal axial yield capacity.

4.1 Stress Distribution

With no axial load applied to the cross-section, it was observed that yielding occurred simultaneously on both sides of the web. However, when the member is subject to significant axial compression, the tension side of the web yields prior to the compression side. This effect is amplified at high levels of axial load and is explained by the stress states shown in Figure 8.

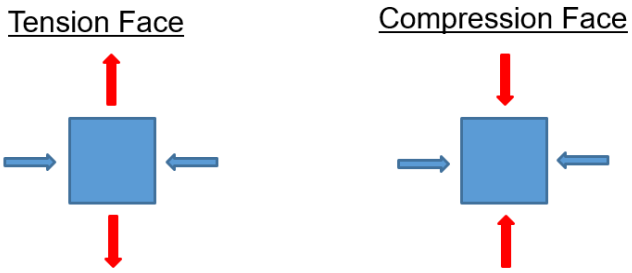

Figure 8: Web Surface Stress State

The force combination on the tension face results in a higher von Mises stress compared to the force combination on the compression face. Therefore, a higher applied moment is required to yield the material on the compression face of the wide-flange column.

Bending stress components were taken from the integration points at the yielding location and plotted through the thickness of the web. All eight integration points in the selected elements showed an effectively linear distribution through the web thickness up to first yield, which is consistent with the assumptions of Equation 5. The yield location is highly localised beneath the pressure loads and is accompanied by high stress gradients in both the longitudinal and through-thickness directions. This results in a notable difference between the values at the element integration points and those at the associated nodes. Given that ABAQUS calculates stress and strain at the integration points and averages them to the surrounding nodes, all values were taken from the integration points rather than the nodes.

4.2 Effective Width

The effective width defined by Equation 2 has been shown to predict the length of web that is mobilized to resist the localised torque accurately when no axial load is present. However, the addition of axial load decreases the bending stress required to cause yielding. The effective width is readily visualized in Figure 9, which plots the bending stress of a W250x89 member at first yield with axial loads ranging from 0 – 75% of its nominal compressive yield capacity. The stress is plotted along the full length of the member at the web surface near the flange–web junction where initial yielding takes place.

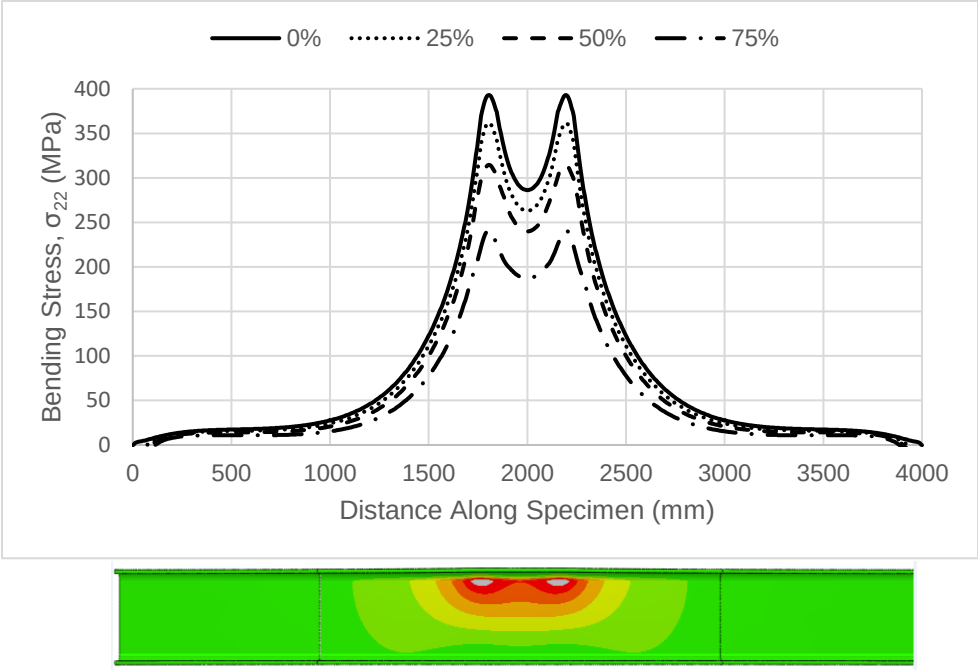

Figure 9: Web Surface Bending Stress at First Yield Under Varying Axial Load (Surface Stress Contour Plot Inset)

A consistent reduction in maximum bending stress (σ_{22}) can be observed as the axial stress in the member increases. This is accompanied by a small reduction in effective width, which is most apparent between 50% and 75% axial load.

4.3 Bending Stress

Table 1 shows a comparison of the bending stress predicted by Equation 5 and the average bending stress obtained from ABAQUS. The reported values were obtained from the integration points at the yield location.

Table 1: Bending Stress Comparison

Section	Axial Load (% of Nominal Yield Capacity)	ABAQUS (MPa)	Equation 5 (MPa)	Equation 5 Error (%)
W250x89	25	348	298	-14.4
	50	303	228	-24.8
	75	225	135	-40.0
W360x91	25	349	298	-14.6
	50	293	228	-22.2
	75	223	135	-39.5
W360x162	25	352	298	-15.3
	50	290	228	-21.4
	75	225	135	-40.0

Equation 5 consistently under-predicts the bending stress mobilized on the tension side of the web at first yield. The difference between the ABAQUS output and predicted values increases with increasing levels of axial load. This discrepancy can be partially explained by investigating the major stress components of a W250X89 member at the yielding location under 0% axial load, as shown in Figure 10.

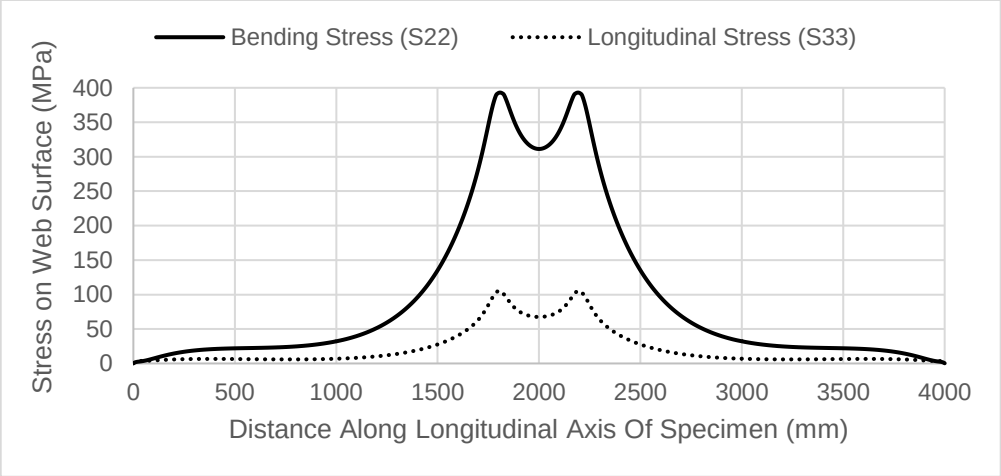

Figure 10: W250x89 Stress Components Under Zero Applied Axial Load

As seen in Figure 10, the bending stress (σ_{22}) exceeds the yield stress of the material (350 MPa) by an appreciable amount and the longitudinal stress (σ_{33}) that can develop is over 100 MPa without any applied axial load. The axial stress is tensile on the tension face of the web, which opposes the bending stress in the von Mises equation, thus allowing more bending stress to develop before yielding occurs. This longitudinal stress develops due to Poisson's ratio interactions. As the torsional moment is applied, if unrestrained the elements on the flexural tension face of the web would undergo elongation in the y-direction (Figure 4), causing contraction in the other two principal directions. However, continuity of the web restrains deformation in the z-direction (Figure 4), causing a longitudinal tensile stress to develop on the critical side of the web.

In order to validate the assumption regarding the longitudinal stress, generalized Hooke's law, given in Equation 6, was evaluated for three models. Individual stress components were taken from the integration points of elements at the yielding location and used to calculate the longitudinal stress that would develop due to Poisson's ratio. These values were compared to the ABAQUS outputs and are summarised in Table 2.

$$[6]\ \varepsilon_{33} = \frac{\sigma_{33}}{E} - \frac{\sigma_{22}\nu}{E} - \frac{\sigma_{11}\nu}{E}$$

ε_{33} = longitudinal strain
σ_{11} = normal stress through web thickness
ν = Poisson's ratio

Table 2: Longitudinal Stress Comparison

Model	ABAQUS (MPa)	Hooke's Law (MPa)	% Difference
W250x89	115.7	118.9	2.75
W360x91	123.6	121.6	1.66
W360x162	116.9	116.2	0.58

The correlation between the hand calculations and numerical results implies that the main source of the longitudinal stress has been accurately identified. Worth noting is that the longitudinal strain (ε_{33}) and through-thickness stress (σ_{11}) account for a very small amount of the overall longitudinal stress. Therefore, its magnitude is largely dependent on the applied bending stress.

5 Conclusion

There is limited research that addresses the behaviour of unstiffened wide-flange members under combined axial load and torsion applied to one flange. The previously proposed method of predicting the strength of these members is unreliable and over-conservative at high levels of axial load. Finite element analysis suggests the bending stress caused by the torsional moment is linear across the web thickness up to initial yielding on the web surface. The empirically-derived effective width term remains relatively constant under varying axial loads. Any reduction in effective width due to high levels of axial load would have limited impact on the overall moment capacity of the member. The shortcoming of Equation 5 appears to be rooted in the stress prediction, which can differ by up to 40% with values obtained numerically. This discrepancy is predominantly attributed to the longitudinal stress that develops due to Poisson's ratio interactions, which was not considered in the proposed method. The findings presented in this paper will be used in combination with the results of an ongoing full-scale laboratory testing program to develop a revised method of predicting the yield moment under this type of combined loading. Accurate identification of this limit is critical to creating simple, cost-effective weak-axis moment connections for use in industrial steel structures.

REFERENCES

Ahmad, M., Driver, R.G., Callele, L., Dowswell, B. 2016. Behaviour of unstiffened wide-flange members subjected to torsional moment through one flange. *Rep No.* 307. University of Alberta, Edmonton, Alberta, Canada.

Dassault Systems. 2014. *ABAQUS/CAE User's Guide v. 6.14*. Providence, RI, USA.